Hydride generation for headspace solid-phase extraction with CdTe quantum dots immobilized on paper for sensitive visual detection of selenium

Huang, Ke; Xu, Kailai; Zhu, Wei; Yang, Lu; Hou, Xiandeng; Zheng, Chengbin

Publisher's version / Version de l'éditeur:
https://doi.org/10.1021/acs.analchem.5b03128
Analytical Chemistry, 88, 1, pp. 789-795, 2015-12-03

analytical chemistry

Article

pubs.acs.org/ac

Hydride Generation for Headspace Solid-Phase Extraction with CdTe Quantum Dots Immobilized on Paper for Sensitive Visual Detection of Selenium

Ke Huang,[†] Kailai Xu,[†] Wei Zhu,[†] Lu Yang,[§] Xiandeng Hou,[*,†,‡] and Chengbin Zheng[*,†]

[†]Key Laboratory of Green Chemistry and Technology of MOE, College of Chemistry, Sichuan University, Chengdu, Sichuan 610064, China

[‡]Analytical & Testing Center, Sichuan University, Chengdu, Sichuan 610064, China

[§]National Research Council Canada, Ottawa, Ontario K1A 0R6, Canada

Supporting Information

ABSTRACT: A low-cost, simple, and highly selective analytical method was developed for sensitive visual detection of selenium in human urine both outdoors and at home, by coupling hydride generation with headspace solid-phase extraction using quantum dots (QDs) immobilized on paper. The visible fluorescence from the CdTe QDs immobilized on paper was quenched by H_2Se from hydride generation reaction and headspace solid-phase extraction. The potential mechanism was investigated by using X-ray diffraction (XRD) and X-ray photoelectron spectroscopy (XPS) as well as Density Functional Theory (DFT). Potential interferences from coexisting ions, particularly Ag^+, Cu^{2+}, and Zn^{2+}, were eliminated. The selectivity was significantly increased because the selenium hydride was effectively separated from sample matrices by hydride generation. Moreover, due to the high sampling efficiency of hydride generation and headspace solid phase extraction, the sensitivity and the limit of detection (LOD) were significantly improved compared to conventional methods. A LOD of 0.1 $\mu g\ L^{-1}$ and a relative standard deviation (RSD, $n = 7$) of 2.4% at a concentration of 20 $\mu g\ L^{-1}$ were obtained when using a commercial spectrofluorometer as the detector. Furthermore, a visual assay based on the proposed method was developed for the detection of Se, 5 $\mu g\ L^{-1}$ of selenium in urine can be discriminated from the blank solution with the naked eye. The proposed method was validated by analysis of certified reference materials and human urine samples with satisfactory results.

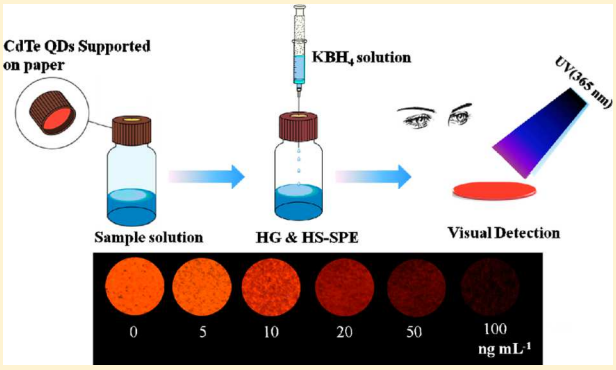

Selenium (Se) is an essential trace element for human and animals because it is one of the constituent elements of antioxidant enzymes, which can protect cells against adverse effects from free oxidative radicals generated from oxygen metabolism. On the other hand, selenium can induce toxic effects at relatively excess intakes.[1−4] The concentration range of selenium between harmful and beneficial to human is very narrow (50−200 μg daily intake).[5] Therefore, the accurate determination of selenium in the human body has attracted considerable interest.[6] Compared to other body fluids, urine is easy to access and analyze. Moreover, the Se-related metabolites in urine such as Se-methylselenogalactosamine, selenosugars, and trimethylselenium are helpful to understand the health benefits ascribed to this element.[7−15] Numerous techniques have been developed to determine selenium concentration in urine.[2,16,17]

Hydride generation (HG) atomic spectrometry is one of the most widely used methods for selenium detection or speciation analysis because of its unmatched sensitivity, efficient separation of matrix and spectral interferences, high analyte transport efficiency, and high selectivity. However, these techniques usually require expensive and bulky atomic spectrometric instruments, and the determination of selenium cannot be accomplished at home or in the field.[18−20] In order to miniaturize the analytical systems, Bendicho et al. have recently developed a quantum dots (QD)-based headspace single-drop microextraction-microfluorospectrometric method for sensitive and selective detection of Se (IV) in water.[21,22] This method not only retained the advantages of HG but also simplified the experimental setup, improved sensitivity, and reduced QDs consumption. Nevertheless, a relatively expensive microfluorospectrometer was still required. In addition, it is not easy to reproduce a drop of several microliters in the headspace, and requires experienced operators to achieve accuracy and reproducibility. Therefore, it is of importance to develop a

Received: August 14, 2015
Accepted: December 3, 2015
Published: December 3, 2015

DOI: 10.1021/acs.analchem.5b03128
Anal. Chem. 2016, 88, 789−795

simple, inexpensive, sensitive, rapid, and equipment-free method for Se detection in the field or at home.[23]

Recently, the paper analytical device (PAD) has drawn much attention in analytical and clinical chemistry by virtue of its versatility, high abundance, and low cost.[23,24] Among various detection methods used in PAD, visual detection based on an enzymatic or chemical interaction has been widely used because of its simplicity, rapidness, disposable, and visual detection with the naked eye.[25] Although many PAD assays were previously developed to quantify biological molecule or toxic metal ions, the use of nanomaterials for development of PAD assays is rather limited[24] besides gold nanomaterials used in PAD assays for visual detection of ions, nucleic acid and cancer cells.[26−30] Semiconductor nanocrystals, especially quantum dots, have been confirmed as an attractive fluorophore for PAD because of its broad absorption spectra, narrow, symmetrical and size-tunable emission spectra as well as long photoluminescence lifetimes (>20 ns), greater photostability and brightness than organic fluorophores.[31,32] Eychmüller et al. first used glutathione capped CdTe quantum dots (QDs) and enzymes encapsulated with poly(diallyldimethylammonium chloride) (PDDA) via electrostatic attraction to form hybrid PAD for the visual detection of phenol (catechol) and glucose.[33] Recently, Krull et al. have presented a paper-based solid phase assay for transduction of nucleic acid hybridization by using immobilized quantum dots (QDs) as donors in fluorescence resonance energy transfer (FRET).[34−36] It is noteworthy that almost all of these PAD assays were accomplished by exposing the PAD to liquid samples without any preconcentration. Therefore, the interferences from sample matrices are inevitable and sensitivities are usually insignificant to analyze real samples.

In this work, a method by coupling QDs based PAD assay with HG for headspace solid phase extraction (HS-SPE) was developed for visual detection of selenium in human urine with the naked eyes. In the proposed method, a gas−solid reaction between the paper supported CdTe QDs and the generated H_2Se occurred to quench the fluorescence of the QDs. Owing to the advantages of efficient matrix separation from HG, the interferences from sample matrices were eliminated, particularly the serious interferences from transition and noble metal ions (such as Ag^+, Cu^{2+}, and Zn^{2+}), which can significantly and rapidly quench the fluorescence via the cation exchange reaction between QDs and metal ions.[37] More importantly, HS-SPE together with visual detection facilitates an easy, sensitive, rapid, and portable detection.

EXPERIMENTAL SECTION

Chemicals. All reagents used in this work were of analytical grade or higher. $Cd(NO_3)_2{\cdot}4H_2O$, KBH_4, $Na_3C_6H_5O_7{\cdot}2H_2O$ from Kelong Reagent Factory (Chengdu, China) and Na_2TeO_3 from Aladdin Reagent Co. (Shanghai, China) were used to prepare CdTe QDs. 3-mercaptopropionic acid (MPA), mercaptosuccinic acid (MSA), L-cysteine (L-cys) and thioglycolic acid (TGA) (Aladdin Reagent Co., Shanghai, China) were used as the capping agents for the QDs. High-purity hydrochloric acid (HCl) and NaOH were from Kelong Reagent Factory (Chengdu, China). The 100 mg L^{-1} of Se(IV) stock solution and 1000 mg L^{-1} stock solutions of Cd^{2+}, As^{3+}, Sn^{4+}, Te^{4+}, Sb^{4+}, Bi^{3+}, Zn^{2+}, Hg^{2+} Na^+, K^+, Mg^{2+}, Ca^{2+}, Cr^{3+}, Ag^+, Fe^{3+}, Mn^{2+}, and Cu^{2+} were from the National Research Center for Standard Materials (NRCSM) of China. High-purity 18.2 MΩ cm deionized water (DIW) obtained from a Milli-Q water system (Chengdu Ultrapure Technology Co., Ltd., Chengdu, China) was used throughout this work.

The accuracy of the proposed method was validated by analysis of Certified Reference Materials (CRMs) obtained from National Research Center of China and National Research Council Canada (NRCC), including human hair powder (GBW07610a), sediment (GBW07311), urine (GBW09102), and dogfish muscle (DORM-2). Microwave digestion of GBW07610a, GBW07311 and DORM-2 was undertaken according to previous work[38] and briefly described in Section 1 of the Supporting Information (SI). Six human urine samples collected from healthy adult volunteers (22 to 30 years old) were used to evaluate this method on real sample analysis.

Instrumentation. A commercial F-7000 spectrofluorometer (Hitachi, Japan) equipped with a solid sensing cell was used to measure fluorescence quenching of the QDs. Absorption spectra were recorded on a UV−vis spectrophotometer (UV-1750, Shimadzu, Japan). High-resolution transmission electron microscopy (HRTEM) images of the QDs were obtained with a Tecnai G^2F20 S-TWIN transmission electron microscope at an accelerating voltage of 200 kV (FEI Co., U.S.A.). Scanning electron microscopy (SEM) was performed with a JSM-7500F scanning electron microscope (JEOL, Tokyo, Japan). The powder X-ray diffraction (PXRD) patterns were obtained from an X'Pert Pro MPD (Philips, Netherlands) using Cu Kα radiation. X-ray photoelectron spectroscopy (XPS, PHI-5000 Versa Probe, ULVAC-PHI) was used to determine the valent state of the QDs obtained after reaction. Fluorescence imaging was carried out with a gel image analysis system (Beijing Liuyi Instrument Factory, WD-9413A) equipped with a 365 nm reflected UV source. A commercial two-channel hydride generation nondispersive atomic fluorescence spectrometer (AFS-9600, Beijing Haiguang Instrumental Co., Beijing, China) fitted with a four-channel peristaltic pump, a quartz gas/liquid separator (GLS), a quartz atomizer, and a coded high intensity selenium hollow cathode lamp was used for the detection of the intensity of the selenium atomic fluorescence.

Synthesis of CdTe QDs. The CdTe QDs were prepared according to a previously reported one-pot synthetic method.[39] Briefly, 0.5 mmol of $Cd(NO_3)_2{\cdot}4H_2O$ and 0.20 g of trisodium citrate dehydrate were dissolved in 50 mL of water, followed by instant addition of 52 μL of MPA (or 16.6 μL TGA, 29.1 μL L-cys and 36.0 mg MSA). The pH of the solution was adjusted to 10.5, followed by the addition of 0.1 mmol Na_2TeO_3 and 50 mg KBH_4, and the resultant solution was refluxed for 1 h. The obtained CdTe QDs solution was precipitated with n-propanol and then centrifuged (11 000 rpm) to remove the supernatant. The purified CdTe QDs were redispersed in double distilled water (DIW). The size and concentration of the CdTe QDs were estimated on the basis of Peng's method.[40] The UV−vis absorption spectra and photoluminescence (PL) emission spectra of the QDs are shown in Figure S1 of the SI.

Preparation of CdTe QDs Impregnated Paper. In order to obtain good reproducibility of preparation of CdTe QDs impregnated paper, the conditions used for preparation of the CdTe QDs must be kept consistent. Meanwhile, chromatography paper obtained from Whatman, U.K. was cut to circular paper sheets with 1 cm in diameter. These paper sheets were immersed in 0.4 μM CdTe QDs solution (10 mL/5 paper sheets) for 30 min and dried in an oven at 40 °C for 30 min.

DOI: 10.1021/acs.analchem.5b03128
Anal. Chem. 2016, 88, 789−795

Scheme 1. Schematic Diagram of the Experimental Setup

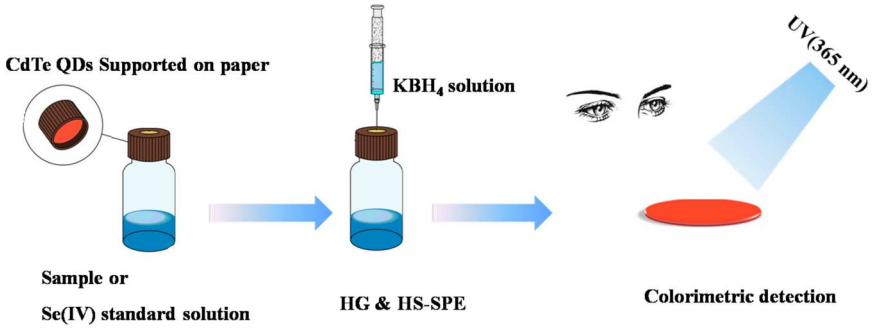

Finally, the paper doped with QDs was then sealed in a plastic bag and kept at 4 °C prior to use.

The fluorescence emission wavelength of CdTe QDs impregnated paper was 650 nm and the quantum yield of the CdTe QDs impregnated paper was evaluated to be 35%.[41]

Analytical Procedure. A schematic of the PAD assay including QDs PAD, HG and headspace SPE is shown in Scheme 1. The paper supported CdTe QDs was adhered to the seal lid of a 25 mL headspace bottle (Hamai Reagent Co., Ningbo, China). Ten milliliters of standard solution of Se (IV) containing 10% (v/v) HCl was added to the bottle and then the bottle was sealed with the lid. One milliliter of 2% (m/v) KBH_4 dissolved in 0.5% (m/v) KOH was injected into the bottle for the generation of H_2Se by HG reaction. The generated volatile Se species were simultaneously headspace extracted and reacted with the CdTe QDs on the paper. The paper was then transferred to a UV test box with 365 nm UV light to accomplish the visual detection of selenium. For the validation of the proposed method on visual detection of selenium in samples, the paper was put into solid sensing cells on a solid sample holder, and their photoluminescence (PL) signals were recorded with the fluorescence spectrometer after reaction and HS-SPE.

RESULTS AND DISCUSSION

Mechanism of the Gas−Solid Reaction between CdTe QDs and H_2Se. As this is the first attempt to develop PAD assay via a gas−solid reaction between QDs and volatile analytes, the initial experiment was to evaluate the feasibility of the proposed PAD assay on quantification of selenium. The paper coated with the CdTe QDs before and after HG and HS-SPE using 50 μg L^{-1} Se(IV) was analyzed by visual detection and fluorescence spectrometric detection, respectively. Figure 1a shows that the fluorescence generated from the QDs with 365 nm UV irradiation is significantly decreased after HG reaction and HS-SPE. The results (Figure 1b) obtained with a commercial spectrofluorometer confirmed this fluorescence quenching effect. In order to gain insight into the mechanism of CdTe QDs fluoresce quenching by H_2Se, characterizations of the CdTe QDs reaction before and after the HG and SPE were carried out by X-ray diffraction (XRD), X-ray photoelectron spectroscopy (XPS) and TEM, as shown in Figure 2. Figure 2a shows that the XRD peaks of CdSe are found in the CdTe QDs immobilized on the paper after the HG and HS-SPE, indicating a reaction between the solid CdTe QDs and gaseous H_2Se that generated CdSe nanomaterials. According to the XPS analysis (Figures 2b and 2c). A Se peak at 53.7 eV of binding energy was observed after the HG and further confirmed the generation of CdSe nanomaterials, which agrees with previous works.[42] The TEM images of the CdTe QDs and its products after reaction indicated the spherical CdTe QDs (Figure 2d) was changed to the random shape (Figure 2e). These observations prove that the surface of CdTe QDs was proportionally covered by CdSe and resulted in the fluorescence quenching.

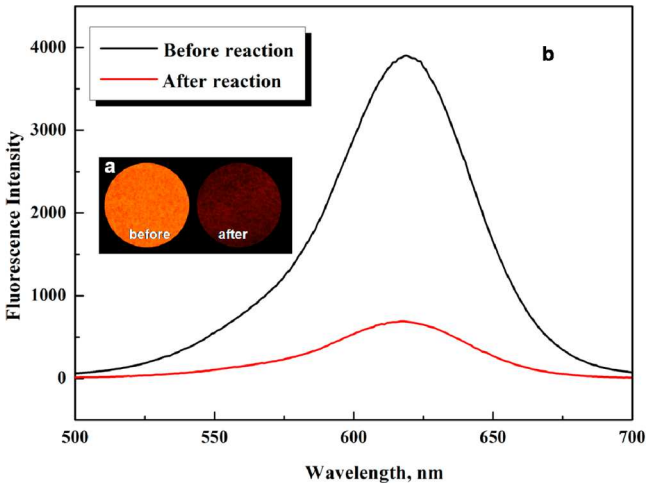

Figure 1. (a) Change of fluorescence of the PAD before and after the HG and SPE; (b) The change of photoluminescence emission spectra of the PAD before and after reaction with 50 μg L^{-1} Se (IV).

Density Functional Theory (DFT) calculations (See Section 3 of the Supporting Information) were also applied here to demonstrate the strong binding affinity between CdTe and H_2Se in the reaction. The adsorption of H_2Se on CdTe QDs was studied by choosing the proper size of $(CdTe)_n$ cluster as a model. Taking the computational efficiency into account, $(CdTe)_n$ (n = 6, 9) were chosen and optimized. The structures of these clusters are shown in Figure 3, similar to previous studies.[43,44] The configurations and adsorption energies are also summarized in Figure 3. The adsorption energy for H_2Se is defined as the following:

$$E_{ads} = E_{adsorbate} + E_{cluster} - E_{adsorbate/cluster}$$

$E_{adsorbate}$ is the energy of free H_2Se, $E_{cluster}$ is the energy of the bare cluster, and $E_{adsorbate/cluster}$ refers to the total energy of the cluster with adsorbates H_2Se. Therefore, the larger positive E_{ads} value, the higher adsorption energy. It should be noted that the adsorption energies of H_2Se on $(CdTe)_6$ and $(CdTe)_9$ are 11.70 and 13.24 kcal/mol, respectively, suggesting that H_2Se should have good binding affinity to the $(CdTe)_n$ clusters. The analysis of mulliken atomic charges indicates that the charge transfer occurred between the H_2Se and the substrate. The

DOI: 10.1021/acs.analchem.5b03128
Anal. Chem. 2016, 88, 789−795

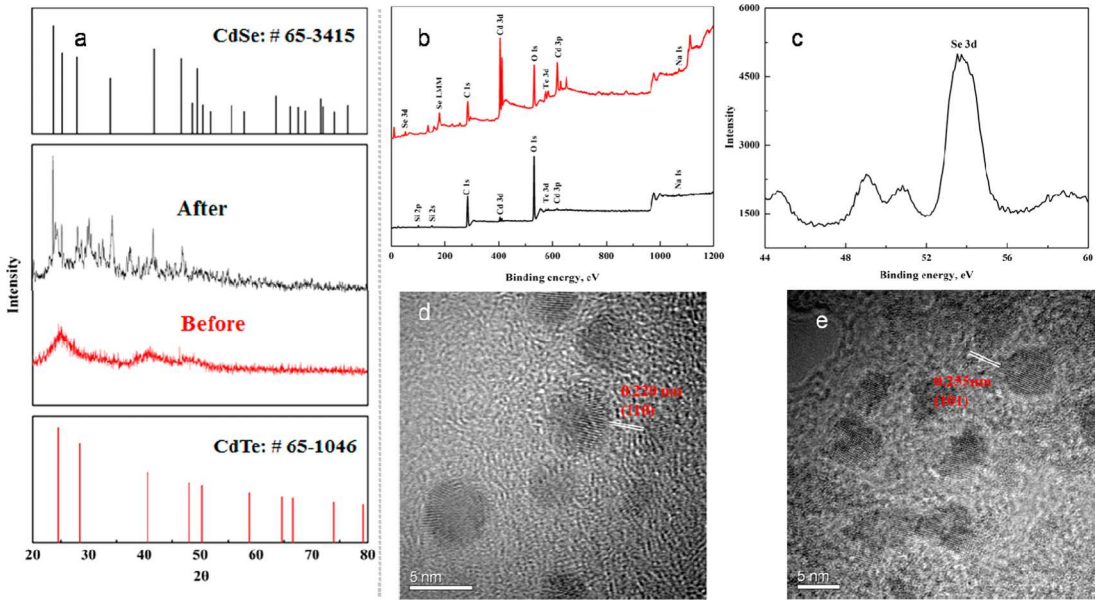

Figure 2. Identification of the reaction in the CdTe PADs with H_2Se. (a) The XRD pattern before and after the reaction; (b) the XPS pattern of the CdTe PAD before (black) and after (red) the reaction; and (c) the Se 3d XPS spectra; The TEM images of CdTe QDs before (d) and after (e) the reaction.

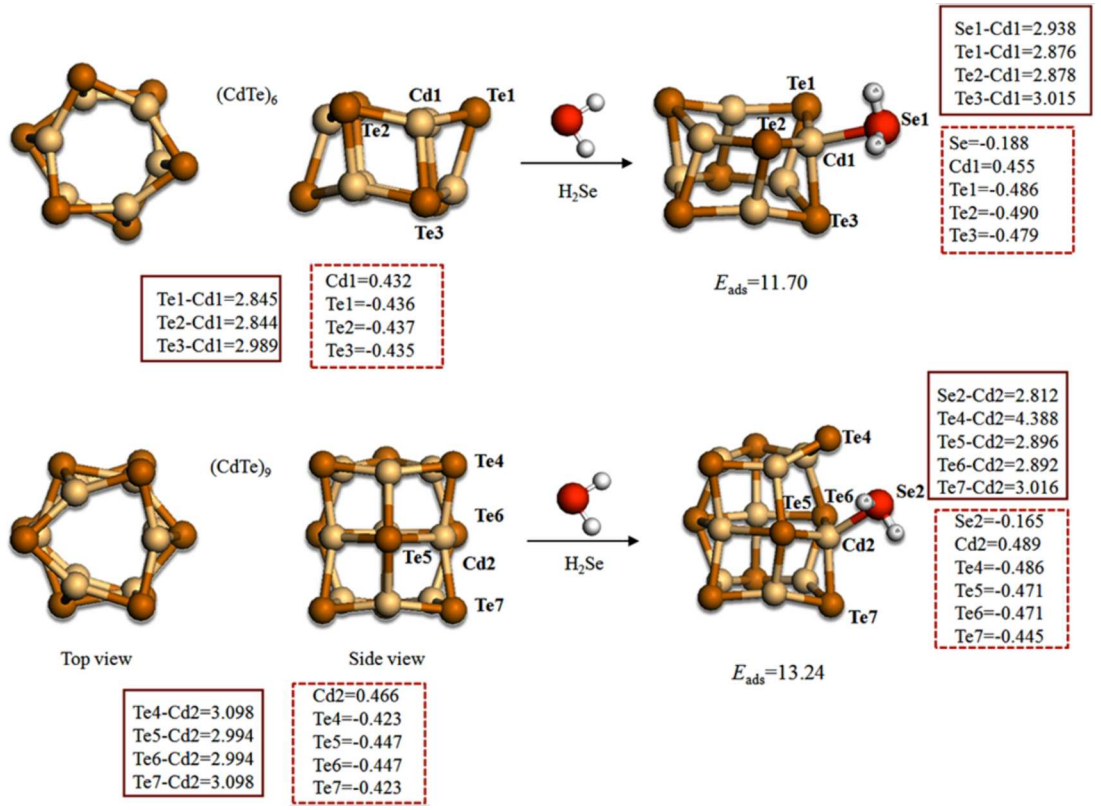

Figure 3. Structures of $(CdTe)_n$ clusters and the adsorption of H_2Se on $(CdTe)_n$ clusters. The Cd, Te, Se, and H atoms are colored in orange, milk-white, red, and white, respectively. The values in solid line rectangle indicate bond lengths. The values in dotted line rectangle indicate mulliken charges. The bond lengths and the adsorption energies are given in angstrom and kcal/mol, respectively.

negatively charged Se and the positively charged Cd infer the attraction between them, such an electrostatic interaction promotes the formation of CdSe species to some extent. The variation of bond lengths also agrees with this trend. After the adsorption of H_2Se, the bond lengths of Cd1−Te3 and Cd2−Te4 are extended to 3.015 Å and 4.388 Å. At the same time, bond lengths of Se1−Cd1 and Se2−Cd2 are 2.938 Å and 2.812 Å, respectively, possessing the properties of a single bond. Previous studies reported[45,46] that a Cd−thiol complex surface layer was created as a shell around the CdTe QDs core to occupy the surface sites and to passivate the QDs. In addition, the binding force of Cd−Se bond was much greater than that of

DOI: 10.1021/acs.analchem.5b03128
Anal. Chem. 2016, 88, 789−795

Cd-thiol. Luminescence decay measurements were performed in the absence and presence of Se(IV). A triexponential luminescence decay (Figure S2) and a decrease of luminescence lifetime with increasing Se(IV) were observed (Table S1), indicating that the mechanism involved in the luminescence quenching is dynamic, and this agrees with previous works.[22,47] On the basis of the above discussions and the previous works,[22,45] we assumed that the binding between Cd in Cd−thiol complex and Se in H_2Se on the surface of CdTe QDs might cause the increase of surface defects thus facilitate the nonradiative e^-/h^+ recombination in the QD surface, which would eventually result in the fluorescence quenching of the CdTe QDs.

Effect of HG Conditions. It is well-known that the HG conditions, including the concentrations of HCl and KBH_4, strongly affect the generation efficiency of H_2Se, thereby influencing the transformation of the CdTe QDs coated on the paper. Therefore, the effect of HCl and KBH_4 concentration on the response from 50 ng mL^{-1} of Se (IV) was evaluated in the range of 1% to 30% (v/v) and 0.5% to 20% (m/v), respectively. The results are summarized in Figures S3a and S3b of the SI. The optimum concentrations of KBH_4 and HCl were found to be 2% (m/v) and 10% (v/v), respectively. Due to the fact that this reaction occurred between gas (H_2Se) and solid phase (QDs), more time was required to complete this reaction. Therefore, the effect of reaction time was also investigated, as shown in Figure S3c. The results indicate a response plateau after 10 min of reaction time.

Effect of CdTe QDs. The ligand has a great effect of the stability in QDs synthesis. CdTe QDs with different ligands such as MPA, MSA, TGA, and L-cys were thus used to investigate this effect. Results in Figure S3d indicate that MPA capped CdTe QDs had the highest sensitivity. In addition, the effect of the concentration of CdTe QDs was investigated by diluting the MPA-stabilized CdTe QDs solution to a range of 0.05 μM to 0.8 μM with DIW. A maximum signal was obtained at the concentration of 0.4 μM. It was reported that QDs usually exhibit size quantization effect, resulting in a red shift of the corresponding fluorescence emission spectral peak with increasing their size.[45] In addition, the size may affect the QDs distribution on the paper and influence the sensitivity of the proposed method. Therefore, the effect of the CdTe QDs size on the QDs distribution and sensitivity was investigated by using the CdTe QDs with particle size in the range of 2−4 nm. The results are shown in Figure S4a and Figure S4b, indicating all the tested QDs with different size can be evenly distributed on the paper and used to sensitively determine selenium. The CdTe QDs doped paper with red fluorescence was chosen for further work because of its better visuality and sensitivity.

Interference and Stability of CdTe QDs Immobilized on Paper. One major shortcoming associated with the conventional QDs-based methods for the determination of analyte ions in liquid phase is the serious interferences from coexisting ions because of the fluorescence quenching caused by the cation exchange reaction between QDs and metal ions. In this study, these effects were not expected to be an issue because selenium was isolated from these ions prior to the fluorescence quenching process. Other possible interferences are from hydride-forming elements, which may cause gas-phase interference during the quenching reaction. Therefore, the effect of 17 diverse ions including hydride forming element ions and transition and noble metal ions were tested, with the results summarized in Table S2 of the SI. As expected, no significant interference from the cation ions (Ag^+, Cu^{2+}, Zn^{2+}, Fe^{3+}, and Mn^{2+}) was detected, even for concentrations as high as 10 mg L^{-1}. The interferences from hydride-forming elements were also not evident, including Cd, As, Sn, Te, Sb, Bi, and Hg. This is probably because that H_2Se is easier to react with Cd of the Cd−thiol complex on the surface of CdTe QDs to form CdSe.[22]

The batch-to-batch accuracy and precision of the assay were also investigated by analyzing 20 μg L^{-1} of Se (IV) with the QD-doped papers prepared from different batches of CdTe QDs. As can be seen from Figure S5 of the SI, good accuracy and precision were obtained.

The lifetime of the PAD was also investigated through the comparison of the responses after reaction with H_2Se obtained from the fresh prepared PAD and the one dried at ambient condition and stored at room temperature for one month, respectively. The results in Figure S6 of the SI were measured by the naked eye and a digital camera, which show that the stability of the PAD was good for the detection of H_2Se even with the storage time as long as one month.

Analytical Figures of Merit. Under optimal conditions, a series of standard solutions containing various concentrations of selenium (0, 5, 10, 20, 50, and 100 μg L^{-1}) were used to evaluate the analytical performance of visual detection of selenium with the proposed PAD assay under 365 nm UV irradiation, as shown in Figure 4. Due to the excellent fluorescent property of the CdTe QDs coated on paper and high efficient preconcentration of HS-SPE, the fluorescence of PAD was quenched gradually by increasing the concentration of Se(IV). Fluorescence quenching was very sensitive, even at the concentration as low as 5 μg L^{-1}, which completely meets the requirement of routine selenium analysis in urine. The analytical figures of merit obtained by using a commercial fluorospectrometer as the detector were established using the Stern−Volmer equation:

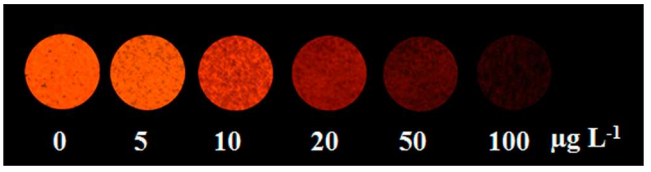

Figure 4. Fluorescence representing the quenching of H_2Se with the concentration of 0, 5, 10, 20, 50, and 100 μg L^{-1}. The images are taken under a 365 nm UV-lamp excitation with a digital camera.

$$I_0/I = K_{SV}[Q] + C \quad (1)$$

where I_0 is the fluorescence intensity of the CdTe QDs based PAD in the absence of H_2Se, I is the fluorescence intensity in the presence of H_2Se, K_{SV} is the Stern−Volmer quenching constant, which is related to the quenching efficiency, and Q is the concentration of Se(IV). As shown in Figure 5, the calibration curve was linear in the range of 5−100 μg L^{-1}, with a linear regression equation of $I_0/I = 0.0905C + 2.7692$. Precision of replicate measurements, expressed as a relative standard deviation (RSD, $n = 7$), is better than 2.4% at a concentration of 20 μg L^{-1}. The limit of detection, defined as the analyte concentration equivalent to 3s (standard deviation) of 11 repeated measurements of a blank solution, is 0.1 μg L^{-1} (1.2×10^{-9} M), about 5-fold better than that obtained by the QDs based headspace single-drop microextraction-microfluorospectrometric method (6.3×10^{-9} M) and comparable to that

DOI: 10.1021/acs.analchem.5b03128
Anal. Chem. 2016, 88, 789−795

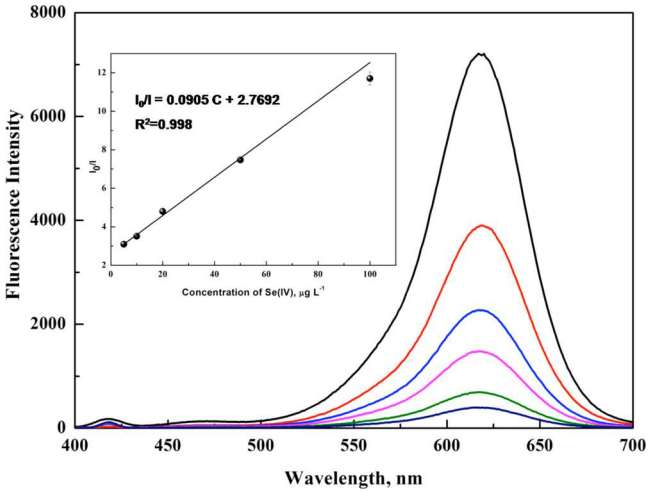

Figure 5. Photoluminescence emission spectra and the corresponding calibration curve of CdTe PADs in the presence of various concentrations of Se(IV).

achieved by conventional ICP-MS. Table S3 summarizes analytical figures of merit achieved using the proposed method and compares with those of several other analytical methods. The LODs of the proposed method are comparable to those obtained by other techniques. Moreover, the proposed method is straightforward, affordable, sensitive, rapid, and equipment-free and enables its end users to conduct visual detection in the field or at home.

Applications. The accuracy of the proposed method was validated by analysis of four CRMs (human hair powder, GBW07610a; urine, GBW09102; sediment, GBW07311; and dogfish muscle, DORM-2) with visual detection and fluorospectrometer, respectively. The results are summarized in Figure 6 and Table 1, which demonstrate the proposed method is capable of producing accurate results for visual detection of selenium in CRMs. The *t* test shows that there is no significant difference between the certified values and the obtained values at the 95% level of confidence. It is worth to note that good recoveries can also be achieved even the sample

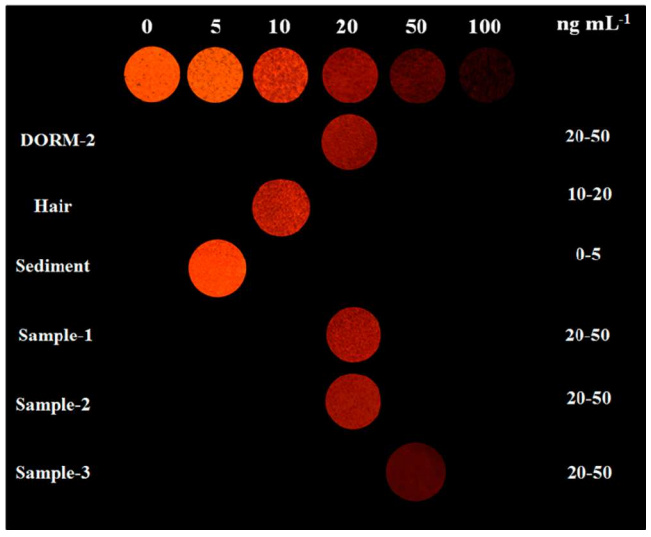

Figure 6. Fluorescence quenching of CdTe PADs for Se(IV) in certified reference samples and human urine samples.

Table 1. Analytical Results for Selenium in Certified Reference Materials

sample	certified value[a] ($\mu g\ g^{-1}$)	detected[a] ($\mu g\ g^{-1}$)	recovery (%)[b]
DORM-2	1.40 ± 0.09	1.48 ± 0.08	105
hair (GBW07610a)	0.60 ± 0.04	0.57 ± 0.03	95
sediment (GBW07311)	0.20 ± 0.06	0.18 ± 0.07	90
urine (GBW09102)	33.7 ± 2.3[c]	31.5 ± 1.6[c]	93

[a]Mean ± SD (n = 3). [b]Calculated by the ratio of detected value and certified value. [c]$\mu g\ L^{-1}$

contained high concentration of transition metal ions such as Fe and Mn. This is probably because only 1 mL of 2% (m/v) KBH_4 solution was injected to react with 10 mL of sample solution containing 10% (v/v) HCl and then the reaction medium can remain at the state with high concentration of inorganic acid to dissolve the metallic state or colloidal forms of Fe and Mn, thereby eliminating their interferences. This viewpoint was confirmed and summarized in Figure S7 of the SI.

To further evaluate the potential application of this PAD visual sensor for indicating the selenium status of the human body, the proposed method was also applied for the detection of Se (IV) in six human urine samples, as shown in Figure 6 and Table 2. The results obtained by fluorospectrometry agree well with those obtained by atomic fluorescence spectrometry, confirming the accuracy of the proposed method.

Table 2. Analytical Results for Selenium in Human Urine Samples Compared with Those by HG-AFS

sample	detected by HG-AFS[a] ($\mu g\ L^{-1}$)	detected by PADs[a] ($\mu g\ L^{-1}$)	recovery (%)[b]
1	22.6 ± 0.3	20.7 ± 1.4	92
2	29.3 ± 1.3	28.9 ± 1.2	99
3	42.5 ± 0.2	40.0 ± 4.1	94
4	32.6 ± 2.0	30.4 ± 3.2	93
5	20.8 ± 0.1	18.3 ± 0.8	88
6	21.3 ± 1.0	22.6 ± 0.4	106

[a]Mean ± SD (n = 3). [b]calculated by the ratio of the value obtained by PADs and those by HG-AFS.

CONCLUSIONS

Hydride generation for headspace solid phase extraction with CdTe quantum dots-immobilized on paper can be used for sensitive visual detection of selenium. Selemium (IV) in human urine can be easily and sensitively detected by the proposed method. This method is straightforward, affordable, sensitive, rapid, and equipment-free and enables its end users to conduct visual detection in the field or at home in the future. Furthermore, this proposed method could be applied in rapid screening analysis biological sample for trace selenium for diagnosing selenium related disease. In addition, it is worthwhile to note that selective determination of the Se-related metabolites can be accomplished in the future when they are separated from other selenium compounds and converted to Se(IV) prior to their analysis by the proposed method.

DOI: 10.1021/acs.analchem.5b03128
Anal. Chem. 2016, 88, 789−795

■ ASSOCIATED CONTENT

Supporting Information

The Supporting Information is available free of charge on the ACS Publications website at DOI: 10.1021/acs.analchem.5b03128.

Sample preparation; photoluminescence emission and UV absorption spectra of MPS-CdTe QDs; density functional theory calculations; photoluminescence decay curves; luminescence lifetime (ns) of CdTe QDs PAD in the absence and presence of different concentrations of Se(IV); effect of hydride generation conditions and ligands of CdTe QDs; effect of CdTe QDs size; test for the interference from various coexistent ions; reproducibility of different batch of CdTe QDs PADs; investigation of lifetime of PAD; interferences of Fe and Mn on the determination of selenium at different concentration of HCl; and comparison of LODs for the detection of Se(IV) by different techniques (PDF)

■ AUTHOR INFORMATION

Corresponding Authors

*E-mail for C.B.Z.: abinscu@scu.edu.cn. Fax and Phone: +86 28 8541 0528.

*E-mail for X.D.H.: houxd@scu.edu.cn.

Author Contributions

The manuscript was written through contributions of all authors. All authors have given approval to the final version of the manuscript.

Notes

The authors declare no competing financial interest.

■ ACKNOWLEDGMENTS

The authors gratefully acknowledge the National Nature Science Foundation of China (No. 21175093) for financial support.

■ REFERENCES

(1) Rayman, M. P. *Proc. Nutr. Soc.* **2005**, *64*, 527−542.
(2) Francesconi, K. A.; Pannier, F. *Clin. Chem.* **2004**, *50*, 2240−2253.
(3) Strauss, E. *Science* **1999**, *285*, 1339.
(4) Clark, L. C.; Combs, G. F.; Turnbull, B. W.; Slate, E. H.; Chalker, D. K.; Chow, J.; Davis, L. S.; Glover, R. A.; Graham, G. F.; Gross, E. G.; Krongrad, A.; Lesher, J. L.; Park, H. K.; Sanders, B. B.; Smith, C. L.; Taylor, J. R. *Jama-J. Am. Med. Assoc* **1996**, *276*, 1957−1963.
(5) Sanz Alaejos, M.; Diaz Romero, C. *Clin. Chem.* **1993**, *39*, 2040−2052.
(6) Gammelgaard, B.; Bendahl, L. *J. Anal. At. Spectrom.* **2004**, *19*, 135−142.
(7) Kuehnelt, D.; Juresa, D.; Francesconi, K. A.; Fakih, M.; Reid, M. E. *Toxicol. Appl. Pharmacol.* **2007**, *220*, 211−215.
(8) Preud'homme, H.; Far, J.; Gil-Casal, S.; Lobinski, R. *Metallomics* **2012**, *4*, 422−432.
(9) Ouerdane, L.; Aureli, F.; Flis, P.; Bierla, K.; Preud'homme, H.; Cubadda, F.; Szpunar, J. *Metallomics* **2013**, *5*, 1294−1304.
(10) Burri, J.; Haldimann, M. *Clin. Chem. Lab. Med.* **2007**, *45*, 895−898.
(11) Ip, C.; Thompson, H. J.; Zhu, Z. J.; Ganther, H. E. *Biochem. Pharmacol.* **2000**, *60*, 2882−2886.
(12) Kokarnig, S.; Kroepfl, N.; Kuehnelt, D.; Francesconi, K. A. *Anal. Methods* **2014**, *6*, 1603−1607.
(13) Bendahl, L.; Gammelgaard, B. *J. Anal. At. Spectrom.* **2004**, *19*, 950−957.
(14) Chan, Q.; Afton, S. E.; Caruso, J. A. *J. Anal. At. Spectrom.* **2010**, *25*, 186−192.
(15) Jager, T.; Drexler, H.; Goen, T. *J. Anal. At. Spectrom.* **2013**, *28*, 1402−1409.
(16) Klein, M.; Ouerdane, L.; Bueno, M.; Pannier, F. *Metallomics* **2011**, *3*, 513−520.
(17) Gammelgaard, B.; Madsen, K. G.; Bjerrum, J.; Bendahl, L.; Jons, O.; Olsen, J.; Sidenius, U. *J. Anal. At. Spectrom.* **2003**, *18*, 65−70.
(18) Deng, D. Y.; Zhou, J. R.; Ai, X.; Yang, L.; Hou, X. D.; Zheng, C. B. *J. Anal. At. Spectrom.* **2012**, *27*, 270−275.
(19) Long, Z.; Luo, Y. M.; Zheng, C. B.; Deng, P. C.; Hou, X. D. *Appl. Spectrosc. Rev.* **2012**, *47*, 382−413.
(20) Long, Z.; Chen, C.; Hou, X. D.; Zheng, C. B. *Appl. Spectrosc. Rev.* **2012**, *47*, 495−517.
(21) Costas-Mora, I.; Romero, V.; Pena-Pereira, F.; Lavilla, I.; Bendicho, C. *Anal. Chem.* **2011**, *83*, 2388−2393.
(22) Costas-Mora, I.; Romero, V.; Pena-Pereira, F.; Lavilla, I.; Bendicho, C. *Anal. Chem.* **2012**, *84*, 4452−4459.
(23) Parolo, C.; Merkoci, A. *Chem. Soc. Rev.* **2013**, *42*, 450−457.
(24) Liana, D. D.; Raguse, B.; Gooding, J. J.; Chow, E. *Sensors* **2012**, *12*, 11505−11526.
(25) Martinez, A. W.; Phillips, S. T.; Butte, M. J.; Whitesides, G. M. *Angew. Chem., Int. Ed.* **2007**, *46*, 1318−1320.
(26) Fang, Z.; Huang, J.; Lie, P.; Xiao, Z.; Ouyang, C.; Wu, Q.; Wu, Y.; Liu, G.; Zeng, L. *Chem. Commun.* **2010**, *46*, 9043−9045.
(27) Liu, G.; Mao, X.; Phillips, J. A.; Xu, H.; Tan, W.; Zeng, L. *Anal. Chem.* **2009**, *81*, 10013−10018.
(28) Mao, X.; Ma, Y.; Zhang, A.; Zhang, L.; Zeng, L.; Liu, G. *Anal. Chem.* **2009**, *81*, 1660−1668.
(29) Mao, X.; Xu, H.; Zeng, Q.; Zeng, L.; Liu, G. *Chem. Commun.* **2009**, 3065−3067.
(30) Ratnarathorn, N.; Chailapakul, O.; Henry, C. S.; Dungchai, W. *Talanta* **2012**, *99*, 552−557.
(31) Nozik, A. J.; Beard, M. C.; Luther, J. M.; Law, M.; Ellingson, R. J.; Johnson, J. C. *Chem. Rev.* **2010**, *110*, 6873−6890.
(32) Jones, M. R.; Osberg, K. D.; Macfarlane, R. J.; Langille, M. R.; Mirkin, C. A. *Chem. Rev.* **2011**, *111*, 3736−3827.
(33) Yuan, J.; Gaponik, N.; Eychmueller, A. *Anal. Chem.* **2012**, *84*, 5047−5052.
(34) Noor, M. O.; Krull, U. J. *Anal. Chem.* **2013**, *85*, 7502−7511.
(35) Noor, M. O.; Shahmuradyan, A.; Krull, U. J. *Anal. Chem.* **2013**, *85*, 1860−1867.
(36) Costas-Mora, I.; Romero, V.; Lavilla, I.; Bendicho, C. *TrAC, Trends Anal. Chem.* **2014**, *57*, 64−72.
(37) Huang, K.; Xu, K.; Tang, J.; Yang, L.; Zhou, J.; Hou, X.; Zheng, C. *Anal. Chem.* **2015**, *87*, 6584−6591.
(38) Zheng, C.; Yang, L.; Sturgeon, R. E.; Hou, X. *Anal. Chem.* **2010**, *82*, 3899−3904.
(39) Sheng, Z.; Han, H.; Hu, X.; Chi, C. *Dalton Trans.* **2010**, *39*, 7017−7020.
(40) Yu, W. W.; Qu, L. H.; Guo, W. Z.; Peng, X. G. *Chem. Mater.* **2003**, *15*, 2854−2860.
(41) Qu, L. H.; Peng, X. G. *J. Am. Chem. Soc.* **2002**, *124*, 2049−2055.
(42) Agostinelli, E.; Battistoni, C.; Fiorani, D.; Mattogno, G.; Nogues, M. *J. Phys. Chem. Solids* **1989**, *50*, 269−272.
(43) Bhattacharya, S. K.; Kshirsagar, A. *Phys. Rev. B: Condens. Matter Mater. Phys.* **2007**, *75*, 3−15.
(44) Kuznetsov, A. E.; Balamurugan, D.; Skourtis, S. S.; Beratan, D. N. *J. Phys. Chem. C* **2012**, *116*, 6817−6830.
(45) Wu, P.; Yan, X. P. *Chem. Commun.* **2010**, *46*, 7046−7048.
(46) Wu, P.; Zhao, T.; Wang, S. L.; Hou, X. D. *Nanoscale* **2014**, *6*, 43−64.
(47) Shen, J. S.; Yu, T.; Xie, J. W.; Jiang, Y. B. *Phys. Chem. Chem. Phys.* **2009**, *11*, 5062−5069.

DOI: 10.1021/acs.analchem.5b03128
Anal. Chem. 2016, 88, 789−795